COMPUTATIONAL CONTINUUM MECHANICS

ВЫЧИСЛИТЕЛЬНАЯ МЕХАНИКА СЛОШНЫХ СРЕД

Computational Continuum Mechanics. 2021. Vol. 14. No. 2. pp. 210-219 DOI: 10.7242/1999-6691/2021.14.2.18

FEATURES OF THE FLOW OF CONCENTRATED SUSPENSIONS OF SOLID PARTICLES

O.I. Skulskiy

Institute of Continuous Media Mechanics UB RAS, Perm, Russian Federation

Concentrated suspensions of solids, widely used in the pharmaceutical, cosmetic and food industries, exhibit complex rheology. In rheometric one-dimensional flows of concentrated suspensions, a smooth or abrupt increase in stresses with a smooth increase in the strain rate intensity can be observed. This is related to the appearance of a first-order phase transition. In our previous work, a phenomenological rheological model of a concentrated suspension of solid particles in a Newtonian dispersion liquid has been developed. This model is characterized by an S-shaped flow curve and describes both continuous and abrupt increases in the stress intensity with a uniform increase in the strain rate intensity. In this work, exact analytical formulas are obtained for the flow velocity profiles of suspensions measured using rotary viscometers. The model proposed earlier is modified to take into account the non-Newtonian properties of the dispersion medium, which demonstrates pseudoplastic properties at low stress intensities and dilatant properties at high stress intensities. Based on the developed numerical model, the features of the flow of highly concentrated suspensions in plane and axisymmetric channels are analyzed. It is shown that in a flat diffuser, in contrast to Newtonian and pseudoplastic fluids, the longitudinal velocity of the suspension slows down near the walls, where the stresses are maximum, and accelerates in the central part of the channel. Calculations for the submerged jet in the area bounded by the walls show that, with an increase in the average velocity of the incoming pure liquid by more than 0.01 m/s, there occurs a local velocity vortex bounded by a layer with high particle concentration and more viscous medium. The concentration of particles inside the vortex is minimal.

Key words: highly concentrated suspensions, rheological model, non-Newtonian dispersion medium, diffusion-convective transfer, numerical solution, plane and axisymmetric flows

1. Introduction

Suspensions of concentrated solid particles are widely used in medicine, perfumery, chemical, oil and gas industries for hydraulic fracturing. A distinctive feature of suspensions of solid particles is a continuous or discontinuous shear thickening –– increase in stresses with an increase in the shear rate. At high particle concentrations, flow jamming can occur.

A large number of publications are devoted to the rheology of concentrated suspensions and the mathematical modeling of their flows [1–18]. Recently, a number of scientific publications have appeared containing the results of experimental studies and theoretical modeling of the rheological properties of highly concentrated suspensions, demonstrating an abrupt stress response to a smooth increase in the shear rate [19–24]. At known stress intensity, the flow curve is unambiguous, but non-monotonic and has an S-shaped form. Such non-Newtonian rheology arises due to the frictional interaction of particles. Additional effects are introduced by the non-Newtonian properties of the pure dispersed phase [25–27]. The simplest model, which takes into account the linear increase in viscosity with increasing average stress, was used in [28], where analytical expressions were obtained for the pressure distribution and longitudinal velocity profile for pressure flow in flat, circular and annular channels with a moving boundary. However, this model is unable to describe the jump-like stress growth in response to an increase in shear rate. In a previous article [29], the author proposed a phenomenological model of a suspension with a Newtonian dispersion phase, which allows one to obtain accurate analytical expressions for the main rheometric flows necessary for the transition from the integral characteristics measured in the experiment to the flow curve, as well as for determining the material constants included in the model.

If the dispersion liquid is non-Newtonian, the suspension exhibits pseudoplastic properties at low deformation rates, and dilatant at high deformation rates. The non-Newtonian rheology of concentrated slurries is the result of competition and balance between hydrodynamic (dissipative)

Email addresses for correspondence: skul@icmm.ru

and thermodynamic (conservative) forces that result in a non-equilibrium microstructure in the flow. Suspensions of solid particles tend to form different structures under mechanical stress.

Figures 1 and 2 show examples of structures at various concentrations and alternating loads from article [32].

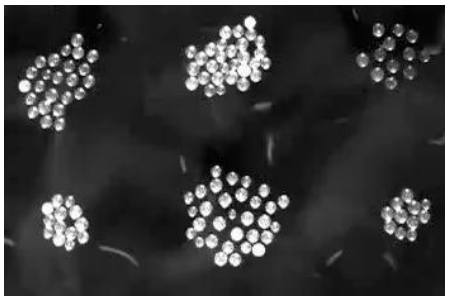

Fig. 1. Clusters formed at a low concentration of particles (the suspension exhibits pseudoplastic properties)

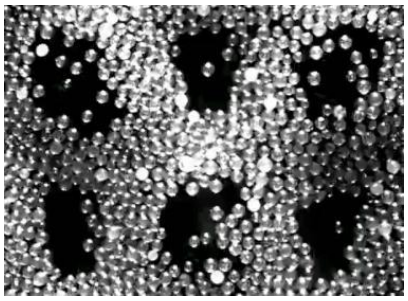

Fig. 2. Anticlusters formed at a high concentration of particles (the suspension exhibits dilatant properties)

Also in article [29], to take into account the non-Newtonian properties of the dispersion medium, a modification of the model is proposed, which consists in adding Ellis's law [2, 10] for the dispersion phase:

$$\eta_{ef} = \frac{\mu_0}{1+a\left(S/S_0\right)^{b-1}} + \eta_0 \left[1+\left(S/S_0\right)^c\right] \Big/ \left(1+\varepsilon\left(S/S_0\right)^c\right), \qquad (1)$$

where $S = \sqrt{\frac{1}{2}\left(\boldsymbol{\tau}:\boldsymbol{\tau}\right)}$ 1: - stress intensity, $\varepsilon = m\frac{\phi^{\bullet}-\phi}{\phi^{\bullet}}$ - parameter, $\phi, \phi^{\bullet}$ - local and limiting concentration, S_0, η_0 μ_0 - characteristic values of stress and viscosity, a, b, c - model parameters, m - fitting parameter. A typical form of the dependence of the effective viscosity on the stress intensity is shown in Figure 2. Model (1) at $\varepsilon = 1$ describes a monotonically decreasing viscosity of the pure dispersion phase. As shown by trial numerical calculations of the plane Poiseuille flow, depending on the value of the applied pressure at the inlet and the parameters of the model, the velocity profiles in the cross section and the shear rate can have various complex shapes.

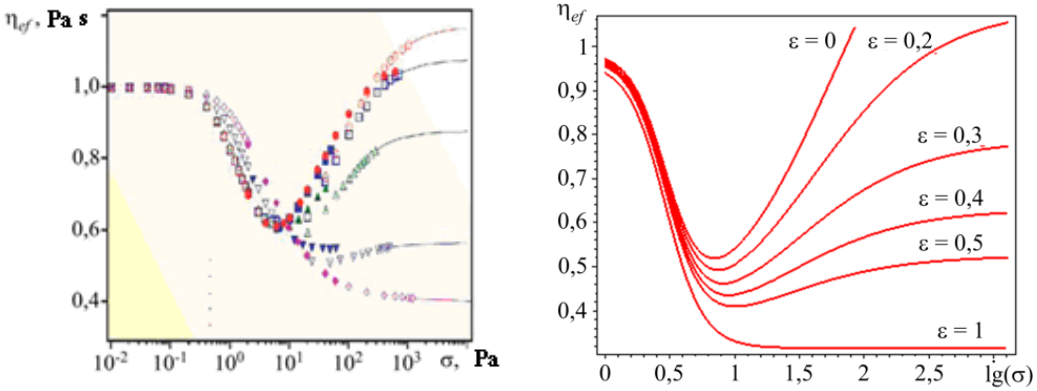

Fig. 3. Typical form of flow curves: experiment (a), calculation by model (1) (b).

The aim of this study is the further development of methods for numerical modeling of two-dimensional problems of the flow of suspensions with an inhomogeneous distribution of the concentration of solid particles.

2. Statement of the problem

In the general case, the flows of concentrated suspensions of solid particles with a non-Newtonian dispersion phase are described by a system of differential equations reflecting the laws of conservation of momentum and mass:

$$\rho\left(\frac{\partial \mathbf{V}}{\partial t}+\mathbf{V}\cdot\nabla\mathbf{V}\right)=-\nabla p+\nabla\cdot\left[\eta_{ef}\left(\nabla\mathbf{V}+\nabla\mathbf{V}^{\mathrm{T}}\right)\right], \tag{2}$$

$$\nabla\cdot\mathbf{V}=0, \tag{3}$$

and convective-diffusion transfer:

$$\left(\frac{\partial \phi}{\partial t}+\mathbf{V}\cdot\nabla\phi\right)=\nabla\cdot\left(\lambda\nabla\phi\right), \tag{4}$$

where t is time, $\mathbf{V}$ is the velocity vector, ∇ is the differentiation operator, p is the pressure (ball part of the stress tensor), η_{ef} is the effective viscosity, ρ is the density, λ is the diffusion coefficient, ϕ is the concentration of particles. System (2) - (4) with rheological equation (1) is closed by the corresponding boundary conditions. Thus, the no-slip conditions for the velocity $\mathbf{V}_{\Gamma}=0$ on fixed walls or the Cauchy conditions for the stresses $\boldsymbol{\sigma}\cdot\mathbf{n}=\mathbf{F}$ at free boundaries are specified. For concentration, conditions of the first $\phi=\phi_{\Gamma}$ or third kind are set $\nabla\phi\cdot\mathbf{n}=h(\phi-\phi^{\bullet})$, where $\mathbf{n}-$ is the normal to the boundary, h is the transfer coefficient).

3. Method of solution

The system of differential equations (2) - (4) is written in the form of Galerkin:

$$\begin{gathered}\int_V \rho\mathbf{U}\cdot\left(\frac{\partial \mathbf{V}}{\partial t}+\mathbf{V}\cdot\nabla\mathbf{V}\right)-\left(\nabla\cdot\mathbf{U}\right)p+\nabla\mathbf{U}:\left[\eta_{ef}\left(\nabla\mathbf{V}+\nabla\mathbf{V}^{\mathrm{T}}\right)\right]dV=\int_S \mathbf{U}\cdot\mathbf{F}\,dS,\\ \int_V \varphi\left(\nabla\cdot\mathbf{V}\right)dV=0,\\ \int_V\left[\chi\left(\frac{\partial \phi}{\partial t}+\mathbf{V}\cdot\nabla\phi\right)+\nabla\chi\cdot\left(\lambda\nabla\phi\right)\right]dV=\int_S \chi\,h(\phi-\phi^{\bullet})dS\end{gathered} \tag{5}$$

where $\mathbf{U}$, φ, χ are weighting functions. To solve the system (5) by the finite element method (FEM), the original FEM FLOW package was used, equipped with a pre- and postprocessor, developed with the participation of the author [35]. The solution was reduced to a sequence of linearized problems, in which nonlinear terms were calculated from the results of previous iterations. At each iteration, discretization of the linearized problems was carried out using triangular finite elements with linear approximation of the components of the velocity and concentration vector, and the pressure was taken piecewise constant within quadrangles consisting of two triangular elements. The convergence of the iterative process was estimated from the effective viscosity, which depends on the local values of concentration and stress intensity and is calculated for each element until the condition is met:

$$\max\left|\frac{\eta_{ef}^{k}-\eta_{ef}^{k-1}}{\eta_0}\right|<\delta$$

where $\delta=10^{-3}$ is a given small number, k is the iteration number.

4. Flow in a flat channel of a suspension with a Newtonian dispersion phase of a known constant concentration

The problems of the flow of a suspension in a flat diffuser at a given constant concentration of particles are solved numerically. The system of equations of the finite element method in the form of Galerkin for a flat channel has the form:

$$\int_0^L\int_0^h \left\{ \rho u_x \left(v_x \frac{\partial v_x}{\partial x} + v_y \frac{\partial v_x}{\partial y} \right) - \frac{\partial u_x}{\partial x} p + \eta_{ef} \left[2 \frac{\partial u_x}{\partial x} \frac{\partial v_x}{\partial x} + \frac{\partial u_x}{\partial y} \left(\frac{\partial v_x}{\partial y} + \frac{\partial v_y}{\partial x} \right) \right] \right\} dxdy = F_x \int_0^h u_x dy ,$$

$$\int_0^L\int_0^h \left\{ \rho u_y \left(v_x \frac{\partial v_y}{\partial x} + v_y \frac{\partial v_y}{\partial y} \right) - \frac{\partial u_y}{\partial y} p + \eta_{ef} \left[2 \frac{\partial u_y}{\partial y} \frac{\partial v_y}{\partial y} + \frac{\partial u_y}{\partial x} \left(\frac{\partial v_y}{\partial x} + \frac{\partial v_x}{\partial y} \right) \right] \right\} dxdy = 0 ,$$

$$\int_0^L\int_0^h \alpha \left(\frac{\partial v_x}{\partial x} + \frac{\partial v_y}{\partial y} \right) dxdy = 0 ,$$

$$\eta_{ef} = \frac{\mu_0}{1 + a\left(S/S_0\right)^{b-1}} + \eta_0 \left[1 + \left(S/S_0\right)^c \right] \Big/ \left(1 + \varepsilon \left(S/S_0\right)^c \right),$$

where v_x, v_y, p - components of the velocity vector and pressure, u_x, u_y, α - weighting functions. In the inlet section of the channel, the surface load F_x was set, in numerical terms equal to the inlet pressure. The adhesion conditions were set on the fixed upper and lower boundaries. Model (1) was used with material constants $\varepsilon = 0,29$, $\phi^{\bullet} = 0,56$, $\mu_0 = 1,34$ $Pa \cdot s$, $\eta_0 = 0,63$ $Pa \cdot s$, $S_0 = 1$ Pa, $a = 40$, $b = 6$, $c = 1$.

The results of calculating the velocity fields of Newtonian, pseudoplastic fluids and suspensions in a flat diffuser on a grid consisting of 50,000 triangular elements are shown in Figure 4.

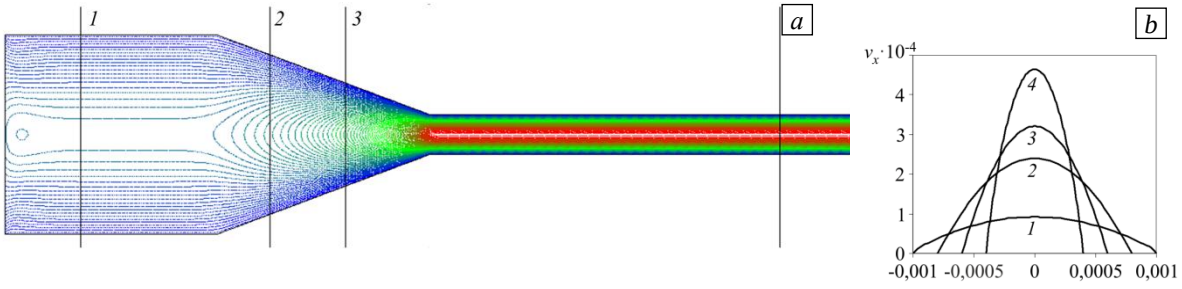

Newtonian fluids $\varepsilon = 1$, $a = 0$, $\mu_0 = 1,34$ $Pa \cdot s$, $\eta_0 = 0,63$ $Pa \cdot s$

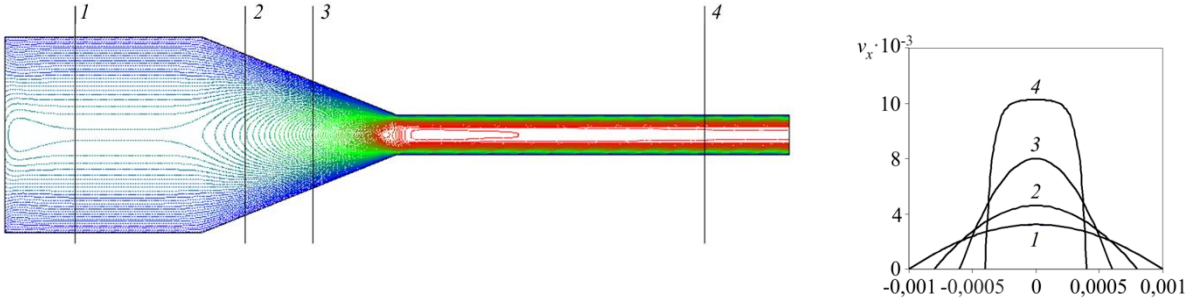

Pseudoplastic fluid $\varepsilon = 1$, $a = 40$, $\mu_0 = 1,34$ $Pa \cdot s$, $\eta_0 = 0,63$ $Pa \cdot s$

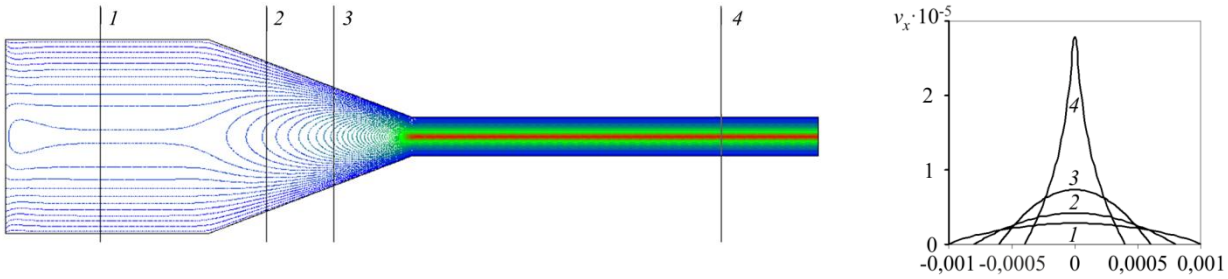

Suspension $\varepsilon = 0,29$, $a = 40$, $\mu_0 = 1,34$ $Pa \cdot s$, $\eta_0 = 0,63$, $Pa \cdot s$

Fig. 4. Isolines of the longitudinal velocity (a) and profiles of the longitudinal velocity along the sections (b).

Note that, in contrast to Newtonian and pseudoplastic fluids, the longitudinal velocity of the suspension slows down near the walls, where the stresses are maximum, and it increases in the central part of the channel.

4. The flow of a suspension with a non-Newtonian dispersion phase in an axisymmetric channel

Let us consider a more complex problem related to the theory of submerged jets [34]. Figure 5 shows a simplified diagram of the device used to study bacterial microflora [30].

Fig.5. Diagram of the device.

The computational domain is represented as a glass with a tube inserted into it, which does not reach the bottom. In the initial state, the space between the glass and the tube is filled with solid particles. Some time after the start of feeding a pure dispersion medium into the tube, under the action of the pressure P_0 applied at the tube inlet or a given average velocity V_0, a certain fraction of the particles is carried out of the region. A layer is formed on the rough inner walls of the channel, which is determined by competing processes: adhesion of particles and their washing away by a stream. As a result, an equilibrium regime is established. In this model, it is assumed that the boundary layers have a constant limiting concentration $\phi^{\bullet}$. The system of equations in the form of Galerkin describing the laminar flow of a suspension in an axisymmetric channel with length L and radii R_z (outer) and $R(0)$ (inner) when solving the problem by the finite element method has the form:

$$2\pi\int_0^L\int_0^{R(z)}\left\{\rho u_r\left(v_r\frac{\partial v_r}{\partial r}+v_z\frac{\partial v_r}{\partial z}\right)+\left(\frac{\partial u_r}{\partial r}+\frac{u_r}{r}\right)p+\eta_{ef}\left[2\frac{u_r v_r}{r^2}+2\frac{\partial u_r}{\partial r}\left(\frac{\partial v_r}{\partial r}\right)+\frac{\partial u_r}{\partial z}\left(\frac{\partial v_r}{\partial z}+\frac{\partial v_z}{\partial r}\right)\right]\right\}rdrdz=0$$

$$2\pi\int_0^L\int_0^{R(z)}\left\{\rho u_z\left(v_r\frac{\partial v_z}{\partial r}+v_z\frac{\partial v_z}{\partial z}\right)+\frac{\partial u_z}{\partial z}p+\eta_{ef}\left[2\frac{\partial u_z}{\partial z}\left(\frac{\partial v_z}{\partial z}\right)+\frac{\partial u_z}{\partial r}\left(\frac{\partial v_r}{\partial z}+\frac{\partial v_z}{\partial r}\right)\right]\right\}rdrdz=2\pi\int_0^{R(0)}u_z F_z\,rdr$$

$$2\pi\int_0^L\int_0^{R(z)}\varphi\left(\frac{v_r}{r}+\frac{\partial v_r}{\partial r}+\frac{\partial v_z}{\partial z}\right)rdrdz=0$$

$$2\pi\int_0^L\int_0^{R(z)}\left\{\chi(v_r\frac{\partial\phi}{\partial r}+v_z\frac{\partial\phi}{\partial z})+\lambda\left(\frac{\partial\chi}{\partial r}\frac{\partial\phi}{\partial r}+\frac{\partial\chi}{\partial z}\frac{\partial\phi}{\partial z}\right)\right\}rdrdz=2\pi\int_0^{R(0)}\chi\alpha(\phi-\phi^{\bullet})\,rdr$$

$$\eta_{ef} = \frac{\mu_0}{1+a\left(S/S_0\right)^{b-1}} + \eta_0\left[1+\left(S/S_0\right)^c\right]\Big/\left(1+\varepsilon\left(S/S_0\right)^c\right)$$

where v_r, v_z, p are the components of the velocity vector and pressure, ϕ is the local concentration of particles, u_x, u_y, φ, χ are the weighting functions, $F_z = P_0$ is the distributed load equal to the pressure at the inlet, $\varepsilon = \dfrac{\phi^\bullet - \phi}{\phi^\bullet}$ parameter that depends on the local concentration of particles. On the channel walls, the no-slip conditions were specified for the velocity, and the boundary conditions of the first kind for the concentration. In the calculations, a model with material constants was used: $\phi^\bullet = 0{,}56$, $\mu_0 = 1{,}34$ $Pa\cdot s$, $\eta_0 = 0{,}63$ $Pa\cdot s$, $S_0 = 1$ $Pa\cdot s$, $a = 40$, $b = 6$, $c = 1$. The calculations were performed on a mesh of 6000 triangular elements. Depending on the parameters of the problem, the convergence of the solution required from 70 to 100 iterations. First, consider the results of calculating the distribution of the main process variables in the channel at a known inlet pressure P_0. Despite the non-monotonic nature of the flow curve, in this case the stress intensity field uniquely determines the strain rate intensity field. Moreover, all the variables shown in Figure 6 behave in a fairly predictable manner. When the velocity of the dispersion medium entering the tube with a nonmonotonic curve is known at the inlet, the flow is fundamentally different from the case considered above. With an S-shaped flow curve, a given strain rate field can cause from one to three states of the stress field that satisfy the equilibrium equations, and one of the states is unstable. Which of the two stable states is realized is determined by prehistory, the role of which is played here by convective transfer.

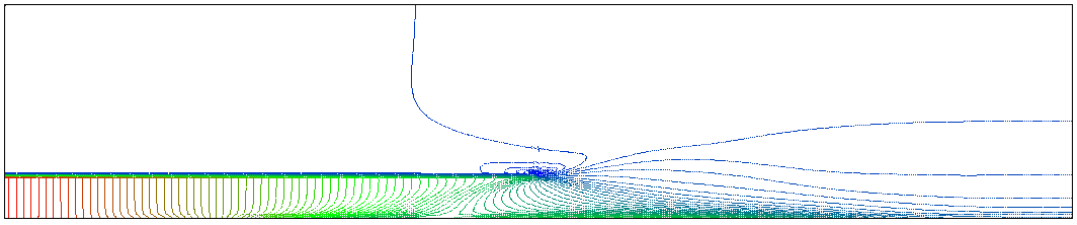

Pressure p

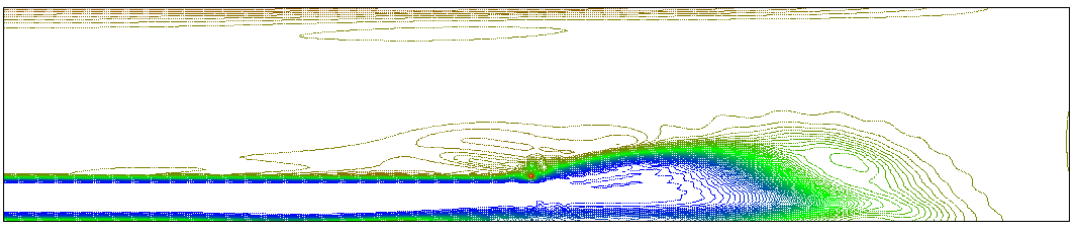

Effective viscosity η_{ef}

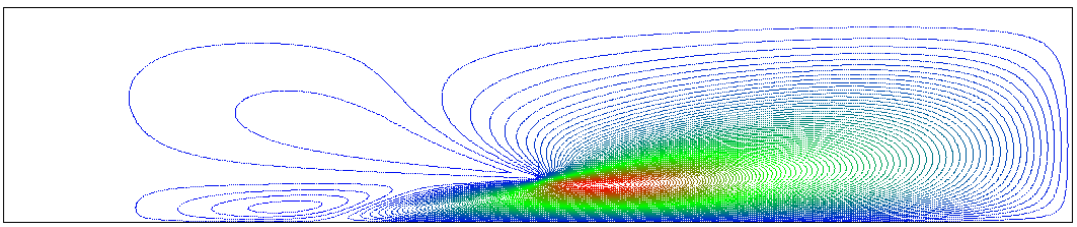

Velocity V_r

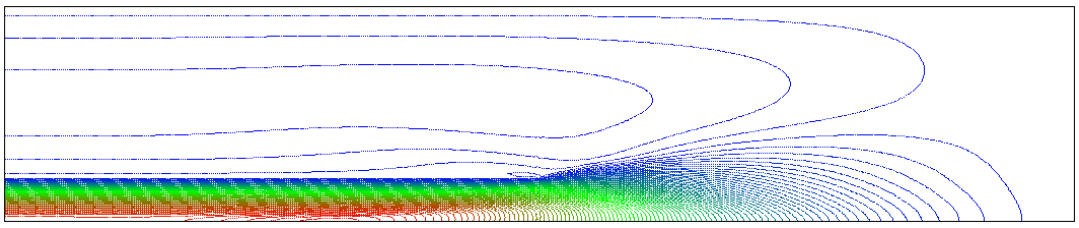

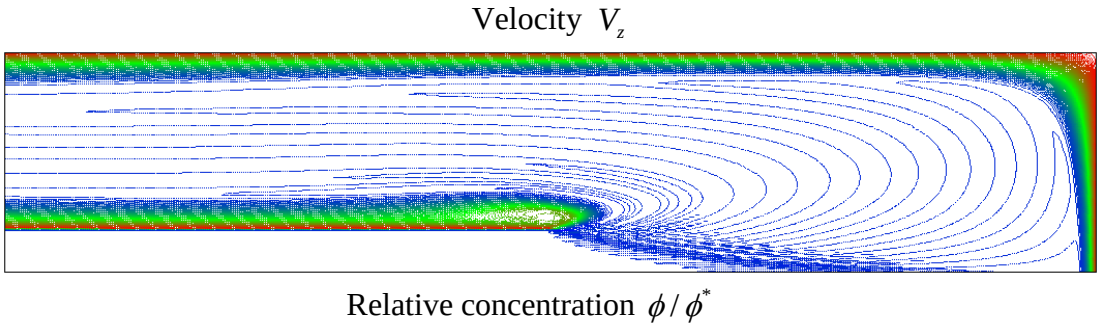

Fig. 6. Distribution of the main variables in the channel at a given inlet pressure.

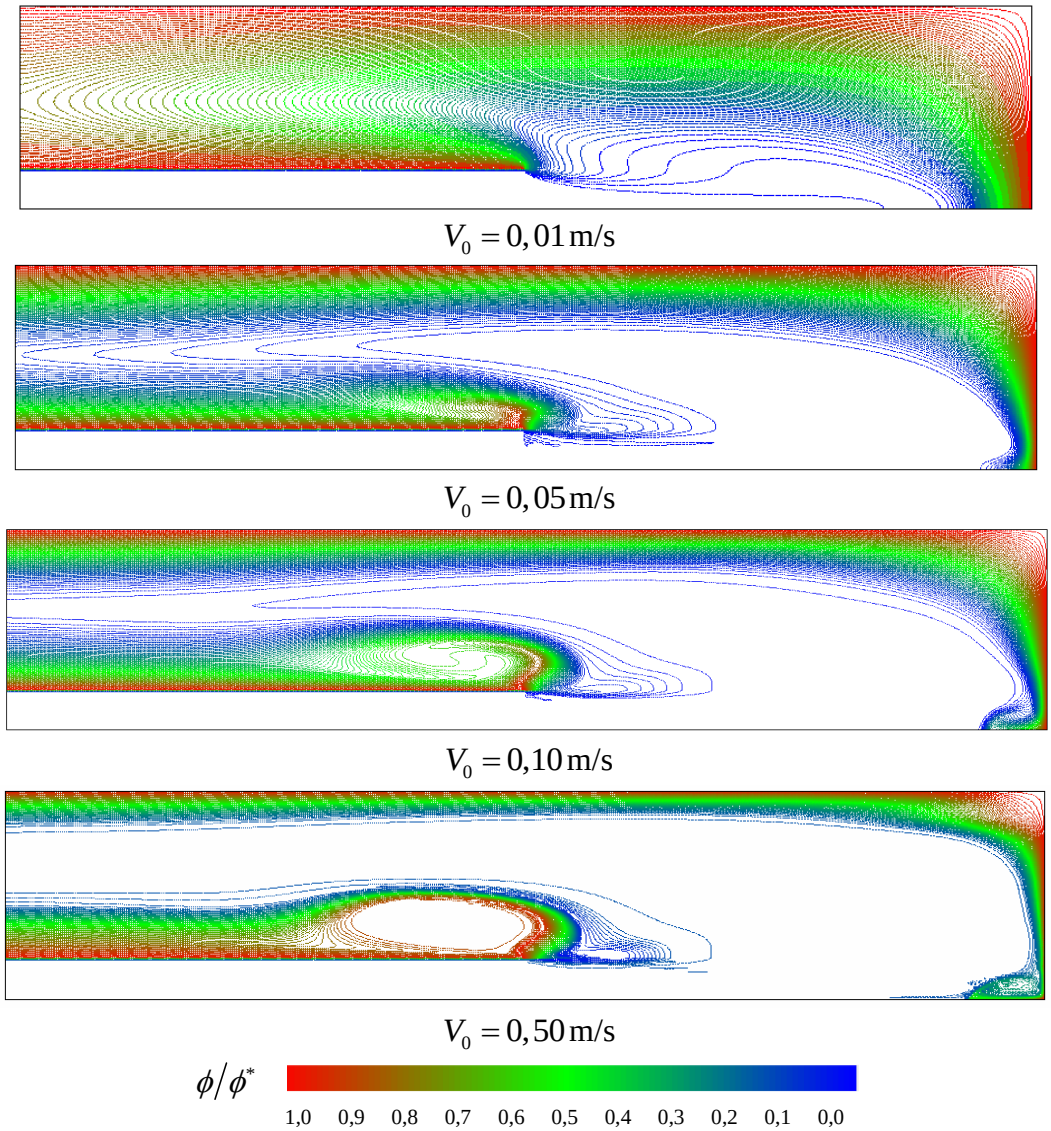

Fig. 7. Distribution of the relative concentration of particles in the channel at a given average injection velocity.

Figure 7 shows the results of calculations of the distribution of the relative concentration of particles in a suspension with a non-Newtonian dispersion medium at different speeds of a pure liquid entering through a tube. Since in the areas of counter flows there are maximum velocity gradients, at the points at which the strain rate intensity exceeds the characteristic value for a given concentration, the stress intensity increases abruptly by 2–3 orders of magnitude. As a result, a layer with an increased viscosity and concentration of particles arises, which, with an increase in the average injection velocity, first bends upward, towards the reverse flow, and then, at a velocity of the incoming pure liquid exceeding 0.1 m/s, a stable anti-cluster is formed - a closed vortex limited

by a layer of highly viscous medium with a high concentration of particles. The concentration inside the vortex is minimal.

6. Conclusion

A numerical model has been developed for quasi-stationary laminar two-dimensional flows of concentrated suspensions with a non-Newtonian dispersion phase and with dilatant properties. On model problems, implemented by the finite element method, the efficiency of the proposed new rheological model of concentrated suspensions is shown, which describes an increase in apparent viscosity with increasing stress intensity. The features of the flow of highly concentrated suspensions in flat and axisymmetric channels are revealed. It is shown that in a flat diffuser, in contrast to Newtonian and pseudoplastic fluids, in a suspension the longitudinal velocity decreases near the walls, where the stresses are maximum, and increases in the central part of the channel. In the model problem of displacing solid particles from a cylindrical glass under the action of a given pressure, despite the non-monotonic nature of the flow curve, the stress intensity field uniquely determines the distributions of the main flow variables. When the average velocity is specified at the tube inlet, the property of non-monotonicity of the suspension flow curve leads to the existence of one to three states of the stress field that satisfy the equilibrium equations, two of which are stable. Which of the stable states will take place is determined by the prehistory, the role of which in this case is played by convective transfer.

As a result of calculations, it was found that with an increase in the velocity of an incoming pure liquid and its excess of 0.01 m/s, the formation of a local vortex with a minimum concentration of particles inside it is observed. The vortex is confined to a layer with a high concentration of particles and a more viscous medium. This phenomenon requires further theoretical research and experimental confirmation.

The study was carried out with the financial support of the Russian Foundation for Basic Research within the framework of scientific project No. 20-45-596020.

References

1. Verdier C. Rheological properties of living materials. From cells to tissues. *J. Theor. Med.*, 2003, vol. 5, pp. 67-91. https://doi.org/10.1080/10273360410001678083
2. Khodakov G.S. Reologiya suspenziy. Teoriya fazovogo techeniya i eye eksperimental'noye obosnovaniye [Suspension rheology. The theory of phase flow and its experimental substantiation]. *Ros. khim. zh. (Zh. Ros. khim. ob-va im. D.I. Mendeleyeva)*, 2003, vol. XLVII, no. 2, pp. 33-43.
3. Guillou S., Makhloufi R. Effect of a shear-thickening rheological behaviour on the friction coefficient in a plane channel flow: A study by direct numerical simulation. *Journal of Non-Newtonian Fluid Mechanics*, 2007, vol. 144, pp. 73-86. https://doi.org/10.1016/j.jnnfm.2007.03.008
4. Galindo-Rosales F.J., Rubio-Hernandez F.J., Velazquez-Navarro J.F. Shear-thickening behavior of Aerosil® R816 nanoparticles suspensions in polar organic liquids. *Rheol. Acta*, 2009, vol. 48, pp. 699-708. https://doi.org/10.1007/s00397-009-0367-7
5. Liu A.J., Nagel S.R. The jamming transition and the marginally jammed solid. *Annu. Rev. Condens. Matter Phys.*, 2010, vol. 1, pp. 347-369. https://doi.org/10.1146/annurev-conmatphys-070909-104045
6. Seth J.R., Mohan L., Locatelli-Champagne C., Cloitre M., Bonnecaze R.T. A micromechanical model to predict the flow of soft particle glasses. *Nature Mater.*, 2011, vol. 10, pp. 838-843. https://doi.org/10.1038/nmat3119
7. Galindo-Rosalesa F.J., Rubio-Hernбndez F.J., Sevilla A. An apparent viscosity function for shear thickening fluids. *Journal of Non-Newtonian Fluid Mechanics*, 2011, vol. 166, pp. 321-325. https://doi.org/10.1016/j.jnnfm.2011.01.001

8. Boyer F., Guazzell E., Pouliquen O. Unifying suspension and granular rheology. *Phys. Rev. Lett.*, 2011, vol. 107, 188301. https://doi.org/10.1103/PhysRevLett.107.188301
9. Nakanishi H., Nagahiro S., Mitarai N. Fluid dynamics of dilatant fluids. *Phys. Rev. E*, 2012, vol. 85, 011401. https://doi.org/10.1103/PhysRevE.85.011401
10. Fortier A. *Mécanique de suspensions* [Suspension mechanics]. Masson et C-ie, 1967. 176 p.
11. Ur'yev N.B. *Fiziko-khimicheskiye osnovy tekhnologii dispersnykh sistem i materialov* [Physicochemical foundations of the technology of dispersed systems and materials]. Moscow, Khimiya, 1988. 255 p.
12. Tanner R.I. *Engineering rheology*. Oxford University Press, 2000. 586 p.
13. Brown E., Jaeger H.M. Shear thickening in concentrated suspensions: phenomenology, mechanisms and relations to jamming. *Rep. Prog. Phys.*, 2014, vol. 77, 046602. http://iopscience.iop.org/0034-4885/77/4/046602
14. Denn M.M., Morris J.F. Rheology of non-Brownian suspensions. *Annu. Rev. Chem. Biomol. Eng.*, 2014, vol. 5, pp. 203-228. https://doi.org/10.1146/annurev-chembioeng-060713-040221
15. Ardakani H.A., Mitsoulis E., Hatzikiriakos S.G. Capillary flow of milk chocolate. *Journal of Non-Newtonian Fluid Mechanics*, 2014, vol. 210, pp. 56-65. https://doi.org/10.1016/j.jnnfm.2014.06.001
16. Mari R., Seto R., Morris J.F., Denn M.M. Nonmonotonic flow curves of shear thickening suspensions. *Phys. Rev. E*, 2015, vol. 91, 052302. https://doi.org/10.1103/PhysRevE.91.052302
17. Pan Zh., de Cagny H., Weber B., Bonn D. S-shaped flow curves of shear thickening suspensions: Direct observation of frictional rheology. *Phys. Rev. E*, 2015, vol. 92, 032202. https://doi.org/10.1103/PhysRevE.92.032202
18. Ness C., Sun J. Shear thickening regimes of dense non-Brownian suspensions. *Soft Matter*, 2016, vol. 12, pp. 914-924. https://doi.org/10.1039/c5sm02326b
19. Vázquez-Quesada A., Ellero M. Rheology and microstructure of non-colloidal suspensions under shear studied with Smoothed Particle Hydrodynamics. *Journal of Non-Newtonian Fluid Mechanics*, 2016, vol. 233, pp. 37-47. https://doi.org/10.1016/j.jnnfm.2015.12.009
20. Nagahiro S., Nakanishi H. Negative pressure in shear thickening bands of a dilatant fluid. *Phys. Rev. E*, 2016, vol. 94, 062614. https://doi.org/10.1103/PhysRevE.94.062614
21. Vázquez-Quesada A., Wagner N.J., Ellero M. Planar channel flow of a discontinuous shear-thickening model fluid: Theory and simulation. *Phys. Fluid.*, 2017, vol. 29, 103104. https://doi.org/10.1063/1.4997053
22. Singh A., Mari R., Denn M.M., Morris J.F. A constitutive model for simple shear of dense frictional suspensions. *J. Rheol.*, 2018, vol. 62, pp. 457-468. https://doi.org/10.1122/1.4999237
23. Singh A., Pednekar S., Chun J., Denn M.M., Morris J.F. From yielding to shear jamming in a cohesive frictional suspension. *Phys. Rev. Lett.*, 2019, vol. 122, 098004. https://doi.org/10.1103/PhysRevLett.122.098004
24. Egres R.G., Wagner N.J. The rheology and microstructure of acicular precipitated calcium carbonate colloidal suspensions through the shear thickening transition. *J. Rheol.*, 2005, vol. 49, pp. 719-746. https://doi.org/10.1122/1.1895800
25. Skulskiy O.I., Slavnov Ye.V., Shakirov N.V. The hysteresis phenomenon in nonisothermal channel flow of a non-Newtonian liquid. *Journal of Non-Newtonian Fluid Mechanics*, 1999, vol. 81, pp. 17-26. https://doi.org/10.1016/S0377-0257(98)00091-3
26. Aristov S.N., Skul'skii O.I. Exact solution of the problem on a six-constant Jeffreys model of fluid in a plane channel. *J. Appl. Mech. Tech. Phys.*, 2002, vol. 43, pp. 817-822. https://doi.org/10.1023/A:1020752101539
27. Aristov S.N., Skul'skii O.I. Exact solution of the problem of flow of a polymer solution in a plane channel. *J. Eng. Phys. Thermophys.*, 2003, vol. 76, pp. 577-585. https://doi.org/10.1023/A:1024768930375

28. Kuznetsova Yu.L., Skul'skii O.I., Sitnikova M.A. Lubricant flow in pressure pipes during wire drawing in a hydrodynamic friction mode. *J. Frict. Wear*, 2007, vol. 28, pp. 359-363. https://doi.org/10.3103/S106836660704006X
29. Skul'skiy O.I. Rheometric flows of concentrated suspensions of solid particles. *Vychisl. mekh. splosh. sred – Computational Continuum Mechanics*, 2020, vol. 13, no. 3, pp. 269-278. https://doi.org/10.7242/1999-6691/2020.13.3.21
30. Fuks N.A. *Mekhanika aerozoley* [Aerosol mechanics]. Moscow, Izd-vo AN SSSR, 1955, 352 p.
31. Gray J.M.N.T. Particle segregation in dense granular flows. *Annu. Rev. Fluid Mech.*, 2018, vol. 50, pp. 407-433. https://doi.org/10.1146/annurev-fluid-122316-045201
32. Sanli C., Lohse D., van der Meer D. From antinode clusters to node clusters: The concentration-dependent transition of floaters on a standing Faraday wave. *Phys. Rev. E*, 2014, vol. 89, 053011. https://doi.org/10.1103/PhysRevE.89.053011
33. Sánchez-Rosas M., Casillas-Navarrete J., Jiménez-Bernal J.A., Kurdyumov V.N., Medina A. *E*xperimental and numerical study of submerged jets from pipes of different wall thicknesses for *Re*<1. *Revista Mexicana de Fisica*, 2020, vol. 66, pp. 69-76.
34. Yavorskiy N.I. *Teoriya zatoplennykh struy i sledov* [The theory of submerged jets and trails]. Novosibirsk, In-t teplofiziki SO RAN, 1998. 242 p.
35. Skul'skiy O.I., Fonarev A.V., Kuznetsova Yu.L. «FEM FLOW» – finite element program for calculating the flow of a viscoelastic fluid in channels with a free surface, taking into account non-isothermal. RF Copyright Certificate No. 2007611760, 25 April 2007.

The authors declare no conflict of interests.
The paper was received on 23.04.2021.
The paper was accepted for publication on 22.05.2021.